INSTITUTE OF PHYSICS PUBLISHING NANOTECHNOLOGY
Nanotechnology **17** (2006) 5260–5263 doi:10.1088/0957-4484/17/20/036

Non-linear operation of nanomechnical systems combining photothermal excitation and magneto-motive detection

Daniel R Koenig, Constanze Metzger, Stephan Camerer and Joerg P Kotthaus

Center for NanoScience and Department für Physik der Ludwig-Maximilians-Universität, Geschwister-Scholl-Platz 1, 80539 München, Germany

Received 13 July 2006, in final form 13 September 2006
Published 3 October 2006
Online at stacks.iop.org/Nano/17/5260

Abstract
We present a non-linear operation of a nanomechanical beam resonator by photothermal excitation at 4 K. The resonators dimensions are 10 μm in length, 200 nm in width, and 200 nm in height. The actuation mechanism is based on a pulsed diode laser focused onto the centre of the beam resonator. Thermally induced stress caused by the different thermal expansion coefficients of the bi-layer system periodically deflects the resonator. Magnetomotively detected amplitudes up to 150 nm are reached at the fundamental resonance mode at a frequency of 8.9 MHz. Furthermore, the third eigenmode of the resonator at a frequency 36 MHz is also excited. We conclude that the photothermal excitation at 4 K should be applicable up to the GHz regime, the operation in the non-linear regime can be used for performance enhancement of nanomechanical systems, and the combination of photothermal excitation and magneto-motive detection avoids undesired cross talk.

(Some figures in this article are in colour only in the electronic version)

1. Introduction

For the last decade, suspended nanoelectromechanical systems (NEMS) have been the subject of intense research and development. NEMS are of high relevance in the area of ultra sensitive applications such as charge, displacement, mass, and even single electron spin detection [1–4]. In highly integrated circuits, they can potentially be utilized as fast switches [5] and frequency filters [6]. Furthermore, they become of great interest in fundamental research as they approach the quantum limit due to continuous miniaturization [7]. Most of these applications are based on dynamic operation, which requires dependable driving mechanisms. Dynamic operation in the non-linear regime can further enhance the performance of nanomechanical systems [8]. A widely used actuation technique meeting this requirement is magneto-motive drive [9]. The functional principle is based on the oscillating Lorentz force a metallized beam resonator experiences in a static magnetic field when an ac-current is sent through it. In the past years, photothermal excitation has been demonstrated to be a reliable alternative driving scheme in ambient conditions [10]. Recently, this was even shown for nanomechanical systems being, in two dimensions, smaller than 300 nm [11].

In this paper, we present non-linear operation of nanomechanical systems by photothermal excitation at 4 K. The devices under test are metallized beam resonators with typical dimensions of 10 μm in length, 200 nm in width, and 200 nm in height. The height of the resonator is composed of 100 nm silicon and 100 nm gold. The mechanical response is probed via magneto-motive detection. The combination of optical excitation and electrical detection has the advantage of decoupling the excitation and probing mechanism, therefore avoiding any undesired cross talk. We show that the affectivity of photothermal excitation at 4 K is comparable to magneto-motive drive. At low temperatures, the driving mechanism should be applicable even to frequencies as high as the GHz range.

2. Experimental setup

The experimental setup is illustrated in figure 1. The beam resonator is placed in a sample tube which is evacuated to

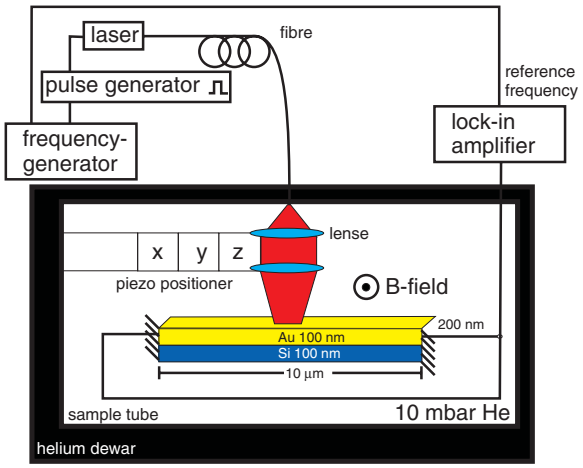

Figure 1. Schematic diagram of laser actuation. A pulsed 10 mW diode laser is focused onto a beam resonator. The laser is modulated by a pulse generator which is triggered by a signal generator. Due to the thermally induced mechanical stress the resonator is actuated. The mechanical response is detected with a lock-in amplifier by measuring the signal caused by the Lorentz force in the magnetic field of 12 T at 4 K.

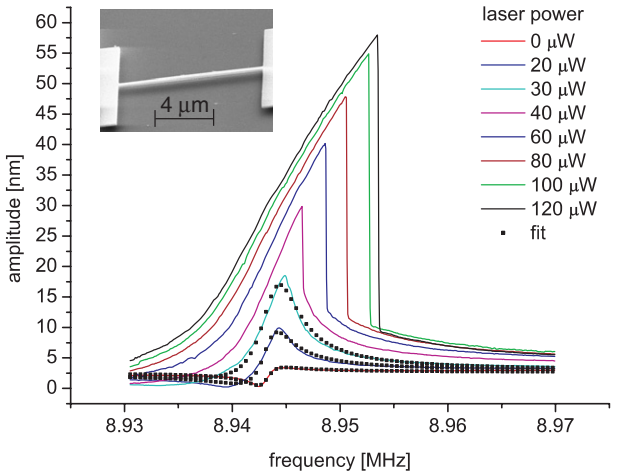

Figure 2. Resonance curves for different laser actuation powers. The beam resonator is driven into the non-linear regime which is described by the Duffing-equation (1). The laser pulse length is set to 55 ns, the magnetic field to 12 T, and the temperature is 4 K. The response of the first three curves fits well to a Lorentzian function with an appropriate phase difference between the driving force and the amplitude response. Inset: SEM image of a doubly clamped free standing Au/Si-bi-layer resonator.

pressures in the 1×10^{-5} mbar range and afterwards filled with 10 mbar of helium, that acts as an exchange gas for cooling. The sample tube is inserted into a 4 K helium bath dewar with a 12 T magnetic field in the sample area. The magnetic field and the low temperatures serve only for detecting the mechanical response of the resonator and are not required for the driving mechanism itself. A 10 mW diode laser with a wavelength of 635 nm is coupled into a single mode fibre. Using a diffraction limited objective mounted on a piezo positioning system (Attocube), the laser is focused onto the centre of the resonator. We estimate the focus diameter to be 500 nm (fwhm). The laser is periodically switched on and off by a square pulse modulation provided by a pulse generator (Philips PM 5712). The pulse generator is triggered by a signal generator (Marconi 2032). The resonator undergoes periodic heating due to the modulated laser irradiation. The thermally induced stress caused by the different thermal expansion coefficients of the bi-layer system periodically deflects the resonator. In conjunction with the magnetic field, the resulting Lorentz force causes a voltage signal proportional to the deflection. The signal is measured with a high frequency lock-in amplifier (Stanford Research Systems SR844).

3. Sample fabrication

The resonators are fabricated from a 5 mm × 5 mm silicon-on-insulator (SOI) chip composed of three layers: a 675 μm silicon substrate (handle), a 500 nm silicon dioxide layer (sacrificial layer), and a 100 nm silicon top layer (device layer). Using electron beam lithography and subsequent thermal evaporation, the metallization is patterned. It consists of a 2 nm titanium adhesion layer, a 100 nm gold layer, and a 30 nm aluminium layer. Next, we utilize reactive ion etching to vertically etch through 100 nm of silicon and into the silicon dioxide layer. The aluminium masks the gold and silicon areas beneath it from the reactive ion etching. In the final wet etch step, we immerse the chip in buffered hydrofluoric acid which selectively etches the sacrificial layer as well as the aluminium mask. The narrow Au/Si-bi-layer features are completely under-etched. These structures become free standing while the wider parts are still supported by the silicon dioxide layer. We are left with suspended metallized beam resonators like the one shown in the scanning electron microscope (SEM) image in the inset of figure 2. The detailed fabrication process is reported in [12].

4. Measurement results and discussion

Finally, the resonators are electrically contacted and placed into the experimental setup. Figure 2 shows a series of resonance curves for different laser powers. The laser power is measured before the laser is coupled into the fibre. We determine that about 50% of the light is lost while transferred through the fibre onto the sample. Considering the focal point of 500 nm (fwhm) diameter, roughly 20% of the laser power is eventually focused onto the resonator. The length of the laser pulses is set to 55 ns, corresponding to about one half of the oscillation period at the resonators fundamental eigenfrequency. We find that this choice of pulse length is most efficient for actuation as illustrated in figure 3. This result is expected since during one half of the period the resonator is moving in the direction of the thermally induced force of the bi-layer system.

For a laser power of higher than 20 μW, the resonator is driven into the non-linear regime [14] described by the Duffing equation:

$$\ddot{x} + 2\gamma\dot{x} + \alpha x + \beta x^3 = \frac{F}{m}\cos(\omega t), \qquad (1)$$

where x is the beam centre amplitude, γ is the damping coefficient, β is the coefficient of non-linearity, F is the

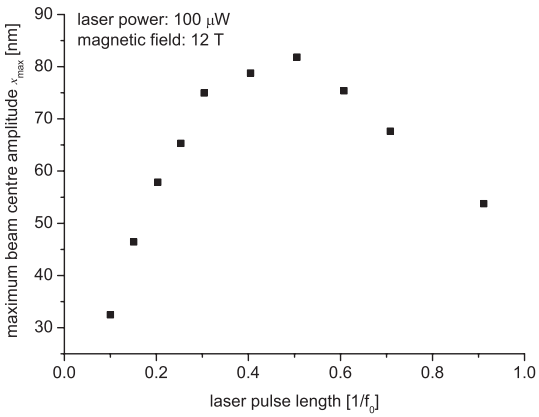

Figure 3. The graph shows the peak amplitude $x_{\max}$ for different laser pulse length, where f_0 is the fundamental eigenfrequency of the resonator. The actuation is most efficient when the pulse length is one half of the period.

effective driving force, and m is the effective mass of the resonator. We establish the relation between the maximum beam centre amplitude and the rms voltage measured by the lock-in amplifier valid for the fundamental resonance mode. We start with the following Maxwell equation:

$$\nabla \times E = -\frac{\mathrm{d}B}{\mathrm{d}t}. \tag{2}$$

Using Stokes-theorem we obtain:

$$V = -\frac{\mathrm{d}\Phi}{\mathrm{d}t} = -B\frac{\mathrm{d}A}{\mathrm{d}t}, \tag{3}$$

where Φ is the magnetic flux, B is the applied magnetic field, and A is the area of the loop through which the magnetic field passes. With equation (3) and the envelope function for the first resonance mode, we calculate V_{rms} and can directly relate the measured lock-in signal to the maximum beam centre amplitude:

$$x_{\max} = \frac{\sqrt{2}V_{\mathrm{rms}}}{(0.5231)\omega l B}, \tag{4}$$

where ω is the frequency of the laser modulation, and l is the length of the beam. Using equation (4), our results show that a maximum amplitude of 150 nm is reached at a laser power of about 310 μW. We would like to note that the resonator with its chip carrier and bond wires will not be perfectly impedance matched to the 50 Ω coax cable which connects the lock-in amplifier to the sample. Therefore, a loss in signal is expected. Hence, our calculated amplitudes should be smaller than the actual ones. This conclusion is supported by equation (5), which approximates the critical amplitude at which the transition from the linear to the non-linear regime occurs [15]

$$x_c = \frac{\sqrt{2}b}{\sqrt{\frac{1}{2}Q(1-\kappa)^2}}, \tag{5}$$

where b is the width of the beam resonator and κ is the Poisson ratio. We approximate κ to be 0.3. From the fit of the resonance curve corresponding to a laser actuation power of 30 μW, $Q = 342$ is obtained. We find x_c to be 30 nm. In comparison, the critical amplitude which is inferred from the non-linear resonance shapes in figure 2 lies below 30 nm corroborating our assumption.

Figure 2 shows that even without optical actuation a signal is detected. This observation is explained by a coherent pick-up (cross talk) from the reference frequency input of the lock-in to the lock-in signal input. The cross talk results in an magneto-motive actuation of the resonator. By fitting the first three curves in figure 2 to a Lorentzian function with an appropriate phase difference between the driving force and the amplitude response, we obtain Q factors of 624 ± 10, 445 ± 10, and 342 ± 10 for laser powers of 0, 20, and 30 μW, respectively. We attribute the decrease in Q factor to a rise in temperature caused by thermal heating of the laser [13]. Using

$$F = \frac{x_{\max} m \omega^2}{Q} \tag{6}$$

with $m = 4 \times 10^{-15}$ kg, $Q = 340$, and $x_{\max} = 150$ nm, we can approximate the effective driving force F to be of the order of 1×10^{-10} N, which is comparable to the effective driving forces for magneto-motive drive.

Probing higher resonance modes by choosing the laser pulse length to be one half of the period of those modes, we are able to excite the third eigenmode at a frequency of 36 MHz. NEMS-beams with higher eigenfrequencies could not be probed with our measurement setup as the pulse generator is limited to a frequency of 50 MHz. In principle, the actuation mechanism should be applicable up to frequencies where the oscillation period becomes comparable with the thermal relaxation time which—for our system—can be estimated as [16, 17]:

$$\tau_{\mathrm{therm}} = \frac{1}{6} l^2 \frac{\rho_{\mathrm{Si}} c_{\mathrm{Si}} + \rho_{\mathrm{Au}} c_{\mathrm{Au}}}{\lambda_{\mathrm{Si}} + \lambda_{\mathrm{Au}}}, \tag{7}$$

where ρ is the density, c is the specific heat capacity, and λ is the thermal conductivity. For 4 K, the thermal relaxation time is of the order of 10 ps so that actuation of frequencies up to the GHz range should be possible. At room temperature, the different thermal conductivity and heat capacity result in a relaxation time of the order of 0.1 μs, which should limit the frequency to about 10 MHz.

For studying the widely observed T dependence of the Q factor, it would be desirable to directly relate temperature, thermal relaxation time, and Q factor. Even though our system may seem adequate for extracting these dependencies, determining the thermal relaxation time still poses a problem. Furthermore, is has to be noted that τ of our system is an effective thermal relaxation time. Because the laser is modulated and focused onto the centre of the resonator, the temperature and therefore also the relaxation time varies locally and over time.

We reliably reproduced the driving mechanism on five resonators. The mechanical response of different samples with the same dimension is not exactly the same. The data of figures 2 and 3 are obtained from two different resonators. The peak amplitudes for a laser power of 100 μW of the two figures do not match due to fluctuations in the fabrication process, uncertainties in the laser focus and position, and timely variations of the laser power which is coupled into the fibre.

5. Conclusion

In conclusion, we present effective photothermal actuation for bi-layer beam resonators at 4 K. The resonators are driven into the non-linear regime with amplitudes up to 150 nm. This is an important feature as non-linear operation can be used for performance enhancement in nanomechanical systems. At 4 K, the driving scheme should be applicable to frequencies as high as the GHz range. The combination of photothermal excitation and magneto-motive detection avoids any undesired cross talk.

Acknowledgments

The authors would like to thank Khaled Karraï for his support and helpful discussions and Stephan Manus for his technical expertise. We gratefully acknowledge financial support by the Deutsche Forschungsgemeinschaft (DFG) under grant KO-416/18-1.

References

[1] Rugar D, Budakian R, Mamin H J and Chui B W 2004 *Nature* **430** 329
[2] Knobel R G and Cleland A N 2003 *Nature* **424** 291
[3] Ilic B, Yang Y and Craighead H G 2004 *Appl. Phys. Lett.* **85** 2604
[4] Cleland A N 2005 *New J. Phys.* **7** 235
[5] Jang J E *et al* 2005 *Appl. Phys. Lett.* **87** 163114
[6] Nguyen C T-C 1999 *IEEE Trans. Microw. Theory Tech.* **47** 1486
[7] LaHaye M D, Buu O, Camarota B and Schwab K C 2004 *Science* **304** 74
[8] Turner Kl, Baskaran R and Zhang 2003 *42nd IEEE Int. Conf. on Decision and Control* vol 3 (Cat.-No. 03CH37475, 2650-1)
[9] Blick R H *et al* 2002 *J. Phys.: Condens. Matter* **14** R905–45
[10] Lavrik N V and Datskos P G 2003 *Appl. Phys. Lett.* **82** 2697
[11] Sampathkumar A, Murray T W and Ekinci K L 2006 *Appl. Phys. Lett.* **88** 223104
[12] Ekinci K L and Roukes M L 2005 *Rev. Sci. Instrum.* **76** 061101
[13] Liftshitz R and Roukes M L 2000 *Phys. Rev.* B **61** 8
[14] Aldridge J S and Cleland A N 2005 *Phys. Rev. Lett.* **94** 156403
[15] Tilmans H A C, Elwenspoek M and Fluitman J H J 1992 *Sensors Actuators* A **30** 35
[16] Gimzewski J K, Gerber Ch, Meyer E and Schlittler R R 1994 *Chem. Phys. Lett.* **217** 589
[17] Barnes J R *et al* 1994 *Rev. Sci. Instrum.* **65** 3793